Available online at www.sciencedirect.com
ScienceDirect
*Chinese Journal of Natural Medicines* 2019, **17**(8): 0575–0584
**Chinese Journal of Natural Medicines**

•Research Articles•

# Differential expression of the *TwHMGS* gene and its effect on triptolide biosynthesis in *Tripterygium wilfordii*

TONG Yu-Ru[1, 2, 3Δ], ZHANG Yi-Feng[3, 4Δ], ZHAO Yu-Jun[2], HU Tian-Yuan[3, 4], WANG Jia-Dian[3, 4], HUANG Lu-Qi[1, 2*], GAO Wei[3, 4, 5*]

[1] *School of Pharmacy Traditional Chinese Materia Medica, Shenyang Pharmaceutical University, Shenyang 110016, China;*
[2] *National Resource Center for Chinese Materia Medica, China Academy of Chinese Medical Sciences, Beijing 100700, China;*
[3] *School of Pharmaceutical Science, Capital Medical University, Beijing 100069, China;*
[4] *School of Traditional Chinese Medicine, Capital Medical University, Beijing 100069, China;*
[5] *Advanced Innovation Center for Human Brain Protection, Capital Medical University, Beijing 100069, China*

Available online 20 Aug., 2019

**[ABSTRACT]** 3-Hydroxy-3-methylglutaryl-CoA synthase (HMGS) is the first committed enzyme in the MVA pathway and involved in the biosynthesis of terpenes in *Tripterygium wilfordii*. The full- length cDNA and a 515 bp RNAi target fragment of *TwHMGS* were ligated into the pH7WG2D and pK7GWIWG2D vectors to respectively overexpress and silence, *TwHMGS* was overexpressed and silenced in *T. wilfordii* suspension cells using biolistic-gun mediated transformation, which resulted in 2-fold increase and a drop to 70% in the expression level compared to cells with empty vector controls. During *TwHMGS* overexpression, the expression of *TwHMGR*, *TwDXR* and *TwTPS7v2* was significantly upregulated to the control. In the RNAi group, the expression of *TwHMGR*, *TwDXS*, *TwDXR* and *TwMCT* visibly displayed downregulation to the control. The cells with *TwHMGS* overexpressed produced twice higher than the control value. These results proved that differential expression of *TwHMGS* determined the production of triptolide in *T. wilfordii* and laterally caused different trends of relative gene expression in the terpene biosynthetic pathway. Finally, the substrate acetyl-CoA was docked into the active site of TwHMGS, suggesting the key residues including His247, Lys256 and Arg296 undergo electrostatic or H-bond interactions with acetyl-CoA.

**[KEY WORDS]** Overexpression; RNAi; HMGS; Triptolide; Acetyl-CoA

**[CLC Number]** R282.5, Q527.1 **[Document code]** A **[Article ID]** 2095-6975(2019)08-0575-10

## Introduction

*Tripterygium wilfordii* (Hook. f.) is a perennial vine plant belonging to the family Celastraceae, which has been widely used to treat rheumatoid arthritis and other inflammatory diseases [1-2]. The medicinal properties of *T. wilfordii* are attributed to terpenes which mainly include di- and triterpenes. Triptolide is a diterpene triepoxide isolated from *T. wilfordii* that exhibits strong antitumor activity. The potential mechanism involves the inhibition of the general RNAPII-mediated transcription [3]. A representative *T. wilfordii* triterpene is the structurally unique celastrol, which hold promise as a powerful anti-obesity agent, a potent anti-inflammatory drug, and a breast cancer treatment [4-6].

Terpenes are derived from the universal C5 precursors isopentenyl diphosphate (IPP) and dimethylallyl diphosphate (DMAPP) [7], which are provided by the mevalonate (MVA) pathway and the 2-methyl-Derythritol-4-phosphate (MEP) pathway [8]. The enzyme 3-hydroxy-3-methylglutaryl-CoA synthase (HMGS) is responsible for the first committed step in the MVA pathway, catalyzing the aldol-type condensation

**[Received on]** 22-Apr.-2019
**[Research funding]** This work was supported by the National Natural Science Foundation of China (No. 81773830), Beijing Natural Science Foundation Program and Scientific Research Key Program of Beijing Municipal Commission of Education (No. KZ201710025022), the Support Project of High-level Teachers in Beijing Municipal Universities in the Period of 13th Five–year Plan (No. CIT&TCD20170324) and National Program for Special Support of Eminent Professionals, and Key project at central government level: The ability establishment of sustainable use for valuable Chinese medicine resources (No. 2060302).
**[*Corresponding authors]** Tel: 86-10-64014411-2955, Fax: 86-10-64013996, E-mail: huangluqi01@126.com (HUANG Lu-Qi); Tel/Fax: 86-10-83916572, E-mail: weigao@ccmu.edu.cn (GAO Wei).
[Δ]These authors contributed equally to the article.
These authors have no conflict of interest to declare.

of acetoacetyl-CoA and acetyl-CoA to 3-hydroxy-3-methyl-glutaryl-CoA (HMG-CoA) [9]. HMGS plays a critical role in the biosynthesis of terpenes in medicinal plants and provides the possibility of regulating the production of target terpene metabolites. The HMGS of *Ginkgo biloba* has been isolated and characterized *via* functional complementation of GbHMGS1 in *Saccharomyces cerevisiae* [10]. An *Escherichia coli* strain that was transformed with a codon-optimized HMGS gene exhibited significantly improved bisabolene production over the control bacteria [11]. LIU *et al.* cloned the full-length cDNA of *TwHMGS* gene and proved that the enzyme participated in yeast terpene biosynthesis in a functional complement assay [12].

However, the unambiguous correlation between *TwHMGS* expression and terpene biosynthesis in *T. wilfordii* has not yet been studied in detail. Overexpression and RNA interference (RNAi) genes encoding the presumptive enzymes directly regulate the transcription levels and change the flux towards the desired end-products. Overexpressing the rate-limiting enzyme HMGR in tobacco (*Nicotiana benthamiana*) led to a 20- to 40-fold increase of sesquiterpenes and a 6-fold increase of triterpenes. The production of $\alpha$-Bisabolol and $\beta$-amyrin finally reached 28.8 and 9.8 mg·g$^{-1}$ dry weight, respectively [13]. Manipulation of *Brassica juncea* HMGS1 in transgenic tomato not only up-regulated several genes related to terpene biosynthesis, but also increased the accumulation of MVA-derived squalene and phytosterols, as well as MEP-derived $\alpha$-tocopherol and carotenoids [14]. It stands to reason that the overexpression of *HMGS* endowed the transgenic tomato plants with a higher terpene accumulation capacity through both MVA and MEP pathways. RNAi provides an effective post-transcriptional silencing method to inhibit the expression of endogenous genes. In this approach, the RNA-induced silencing complex, an siRNA-containing effector complex, recognizes and cleaves the complementary target RNAs [15].

In this study, we analyzed the phylogenetic position of *TwHMGS*. Furthermore, *TwHMGS* was overexpressed and silenced using RNAi in *T. wilfordii* suspension cells. The expression of relevant genes in the terpene biosynthetic pathway and accumulation of triptolide and celastrol were analyzed in the *TwHMGS* overexpression and RNAi groups. The increase and decrease of triptolide content was consistent with the up- and downregulation of *TwHMGS*, suggesting that the encoded enzyme plays an important role in the biosynthesis of this important bioactive molecule. On the basis of molecular docking, we obtained the binding state of the TwHMGS complex with acetyl-CoA and analyzed key residues around the substrate which were suggested to participate in the acetylation/deacetylation, condensation/cleavage and hydrolysis/dehydration processes of the catalytic reaction [16]. Thess findings add to the fundamental knowledge of HMGS and the production of terpenes with pharmacological properties.

## Materials and Methods

### *Suspension cells*

The *T. wilfordii* suspension cells used in this study were cultured as previously reported [17].

### *Bioinformatics analysis*

The phylogenetic analysis of TwHMGS and other HMGSs from diverse species was conducted using MEGA 5.1 software (Arizona State University, USA). The multiple alignment analysis of TwHMGS and nine other HMGSs was especially performed using ClustalW2 (https: //www.ebi.ac.uk/Tools/msa/clustalw2/) and ESPript 3 (http: //espript.ibcp.fr/ESPript/ESPript/). The nine HMGSs from different species were obtained in PDB (http: //www.rcsb.org/).

### *Construction of the entry- and expression vectors*

The entry vectors were constructed using pENTR™/D-TOPO® Cloning Kit (Invitrogen, USA). The overexpression fragment corresponded to the open reading frame (ORF) of *TwHMGS*, while the RNAi fragment contained a specific 515 bp fragment from 880−1394 bp of the *TwHMGS* ORF. All the primers were designed using Primer Premier 5.0 software (PREMIER Biosoft, Canada). Both the overexpression fragment and RNAi fragment were amplified using Phusion High-Fidelity DNA Polymerase (New England Biolabs, USA), with the *TwHMGS* plasmid being as the template. Subsequently, the purified target fragments were ligated into the pENTR™/D-TOPO entry vector according to the manufacturer's instructions (Invitrogen, USA). The entry vectors pENTR−$TwHMGS_{OE}$ and pENTR−$TwHMGS_{Ri}$ were confirmed by sequencing.

The expression vectors were constructed using Gateway LR Clonase™ II Enzyme Mix (Invitrogen, USA). The reaction mixture was composed of pENTR−$TwHMGS_{OE}$ (100 ng), pH7WG2D (150 ng), 1 μL of LR Clonase, and 0.6 μL of TE buffer (pH 8.0). The reaction was carried out at 25 °C for 2 h, after which 0.5 μL of Proteinase K Solution was added and incubated at 37 °C for 10 min. pENTR−$TwHMGS_{Ri}$ and pK7GWIWG2D were used to construct the RNAi expression vector. After screening and sequencing, the recombinant expression vectors pH7WG2D−$TwHMGS_{OE}$ and pK7GWIWG 2D−$TwHMGS_{Ri}$ were enriched and extracted using EZNA® Plasmid Maxi Kit (Omega Bio-tek Inc., USA).

### *Genetic transformation of T. wilfordii suspension cells using a biolistic-gun*

The *T. wilfordii* suspension cells were cultured in MS solid medium. We used a PDS, 100/He gene gun (Bio-Rad, USA) to deliver the expression vectors pH7WG2D−$TwHMGS_{OE}$ and pK7GWIWG2D−$TwHMGS_{Ri}$ mixed with 1 μm gold micro-particles into the *T. wilfordii* suspension cells. The empty vectors pH7WG2D and pK7GWIWG2D were also performed as negative controls. The detailed protocol has been published previously [18]. Each vector transformation was performed in five biological replicates.

### *Verification of successful transformation with the expression vectors*

After genetic transformation, the suspension cells were cultured for 5−7 days to allow sufficient gene expression and metabolite accumulation. To verify the successful transforma-

tion, total RNA of suspension cells was isolated from the suspension cells using the Total RNA Extraction Kit (Promega, Shanghai, China), after which the RNAs were reverse-transcribed to first-strand cDNAs as templates for PCR using the FastQuant RT kit (with gDNase, Tiangen Biotech, Beijing, China). The pH7WG2D vector encodes hygromycin resistance (Hyg) and spectinomycin resistance, while the pK7G WIWG2D vector contains a kanamycin resistance (Kan) cassette. Specific primers were designed to amplify the Hyg fragment and the Kan fragment with the cDNA as templates. The PCR products were detected by gel electrophoresis to verify the successful transformation of the suspension cells with the expression vectors.

*Transcriptional expression analysis of TwHMGS and other selected genes*

Transcript levels of *TwHMGS* and a number of other relevant genes were analyzed using real-time quantitative polymerase chain reactions (RT-qPCR). The LightCycler 480 II (Roche, Switzerland) and KAPA SYBR® FAST qPCR Master Mix Kit (KAPA Biosystems, USA) were used to carry out the expression analysis. The house-keeping gene *β*-actin was used as internal control in each reaction. The RT-qPCR primers for *TwHMGS*, *TwHMGR*, *TwDXS*, *TwDXR*, *TwMCT*, *TwGGPS*, and *TwTPS7v2* are listed in Supplementary Table. The RT-qPCR reaction mixture contained 10 μL of 2 × qPCR Master Mix, 1 μL of cDNA (10 ng), and 0.4 μL of primers (10 μmol·L$^{-1}$) and 8.2 μL of dd$H_2O$. The RT-qPCR conditions encompassed enzyme activation for 3 min at 95 °C, followed by denaturation for 3 s at 95 °C, annealing, extension and data acquisition for 30 s at 60 °C. These conditions were repeated for 40 cycles. Each sample was run in triplicate to reduce data errors, and the relative expression levels were calculated using the $2^{-\triangle\triangle Ct}$ method.

*Extraction and determination of biologically active terpenes in T. wilfordii*

The remaining suspension cells were ground into powder in liquid nitrogen and freeze-dried for 36 h. Approximately 20 mg dry powder were weighed and soaked in 1 mL of 80% (*V*/*V*) methanol overnight at 4 °C, followed ultrasonication at 60 kHz and 25 °C for 30 min. Subsequently, the supernatant obtained by centrifugation at 12 000 *g* for 10 min was filtered through a 0.22 μm PTFE microporous membrane. The contents of triptolide and celastrol were determined using an ACQUITY UPLC™ I-Class System (Waters, Milford, MA, USA) that included a PDA detector. An ACQUITY UPLC HSS T3 chromatographic column (1.8 μm, 2.1 mm ×100 mm, Waters, USA) was used to separate ingredients, keeping the column temperature at 40 °C. The mobile phase was a mixture containing 0. 1% (*V*/*V*) formic acid in acetonitrile (mobile phase A) and 0.1% (*V*/*V*) formic acid in water (mobile phase B). The elution programme comprised 30% (A) at the beginning, 30%−35% (A) at 0−5 min, 35% (A) at 5−8 min, 35%−70% (A) at 8−15 min, 70%−90% (A) at 15−21 min, 90% (A) until 24 min, and the flow rate was set at 0.4 mL·min$^{-1}$. The standard triptolide (> 98%, DESITE, China) and celastrol (> 98%, DESITE, China) were used to generate standard curves to quantify their contents in each suspension cells. The standard curve was plotted by corrected peak area (*Y*) for every standard against its concentration (*X*/mg·L$^{-1}$), generating relative equations to quantify the triptolide and celastrol.

*Molecular docking of TwHMGS-ligand complexes*

The HMGS from *Brassica juncea* is the only plant-derived HMGS with an available crystal structure. Thus, the model structure of TwHMGS was constructed using the SWISS Model (https: //swissmodel.expasy.org/) with *Bj*HMGS (PDB: 2FA3) as the template. The value of GMQE and identity calculated by SWISS Model proved the reliability of modeling. The 2D structure of the substrate acetyl-CoA was downloaded from PubChem (https: //pubchem.ncbi.nlm.nih.gov/compound/acetyl-CoA) and refined using the elbow program in the PHENIX suite. Then, the acetyl-CoA was prepared and docked to the receptor grid of the prepared TwHMGS as described previously [19]. The analysis of the docking result was performed in PyMOL (DeLano Scientific LLC, USA).

## Results

*Sequence analysis of TwHMGS*

TwHMGS catalyzes the first committed step of the MVA pathway for terpene biosynthesis in *T. wilfordii*. The MVA pathway genes which were derived from archaeal evolved through lateral transfer from bacteria and other domain of life [20]. The evolutionary position of TwHMGS was exhibited in a phylogenetic tree of the HMGSs from various species (Fig. 1). The TwHMGS has arisen from a common ancestral gene that evolved into the five groups of enzymes from bacteria, animals, fungi, angiosperms and gymnosperms, which suggests an evolutionary relationship from lower organisms to higher organisms. In the angiosperm group, TwHMGS was 81.74% identical to *Camptotheca acuminata* HMGS [21].

To date, the crystal structures of nine HMGSs have been reported, including those from *Homo sapiens*, bacteria and plant [22-24]. To explore the probable relationship of function and secondary structure, we aligned the sequence of TwHMGS with the nine known HMGSs. The details of secondary structures elements were shown in Fig. 2. Multiple sequence alignment among the HMGS from *Brassica juncea* showed 81% identity, from bacteria for *Myxococcus xanthus* (strain DK 1622), *Enterococcus faecalis*, *Moorea producens* 3L, showed 28.36%, 24.25% and 19.20% identity, respectively, from *Homo sapiens* exhibited 46.65% identity.

*Verification of successful transformation with the expression vectors*

The *TwHMGS* overexpression vector harbored the ORF fragment of *TwHMGS* with 1398 bp, while the RNAi expression vector contained partial fragment of *TwHMGS* with 515 bp. Electrophoresis of the target bands was shown in Fig. 3B.

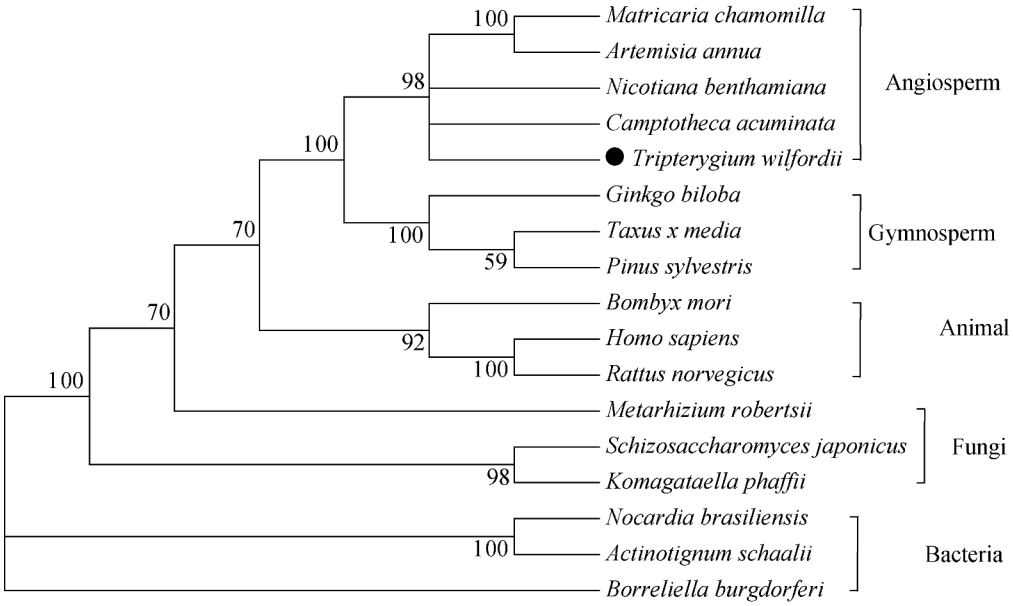


**Fig. 1 Phylogenetic analysis of the amino acid sequence of HMGS from different species. The Neighbor-Joining phylogenetic tree was constructed using the bootstrap method in MEGA 5.1 and the number of Bootstrap replications was 1000. The protein sequences used in the tree are as follows. Bacteria: *Borreliella burgdorferi* CA382 (AGS66682.1), *Nocardia brasiliensis* ATCC 700358 (AFU04599.1), *Actinotignum schaalii* (AIE81946.1); Animals: *Homo sapiens* (AAB72036.1), *Bombyx mori* (BAF62107.1), *Rattus norvegicus* (AAA41336.1); Fungi: *Schizosaccharomyces japonicus* yFS275 (XP_002175595.2), *Komagataella phaffii* CBS 7435 (SCV12104.1), *Metarhizium robertsii* (EXV00357.1); Angiosperms: *Camptotheca acuminata* (ACD87446.1), *Matricaria chamomilla* (AMN10095.1), *Nicotiana benthamiana* (BBE00752.1), *Artemisia annua* (PWA96733.1); Gymnosperms: *Taxus x media* (AAT73206.1), *Ginkgo biloba* (AUW64606.1), *Pinus sylvestris* (CAA65250.1)**

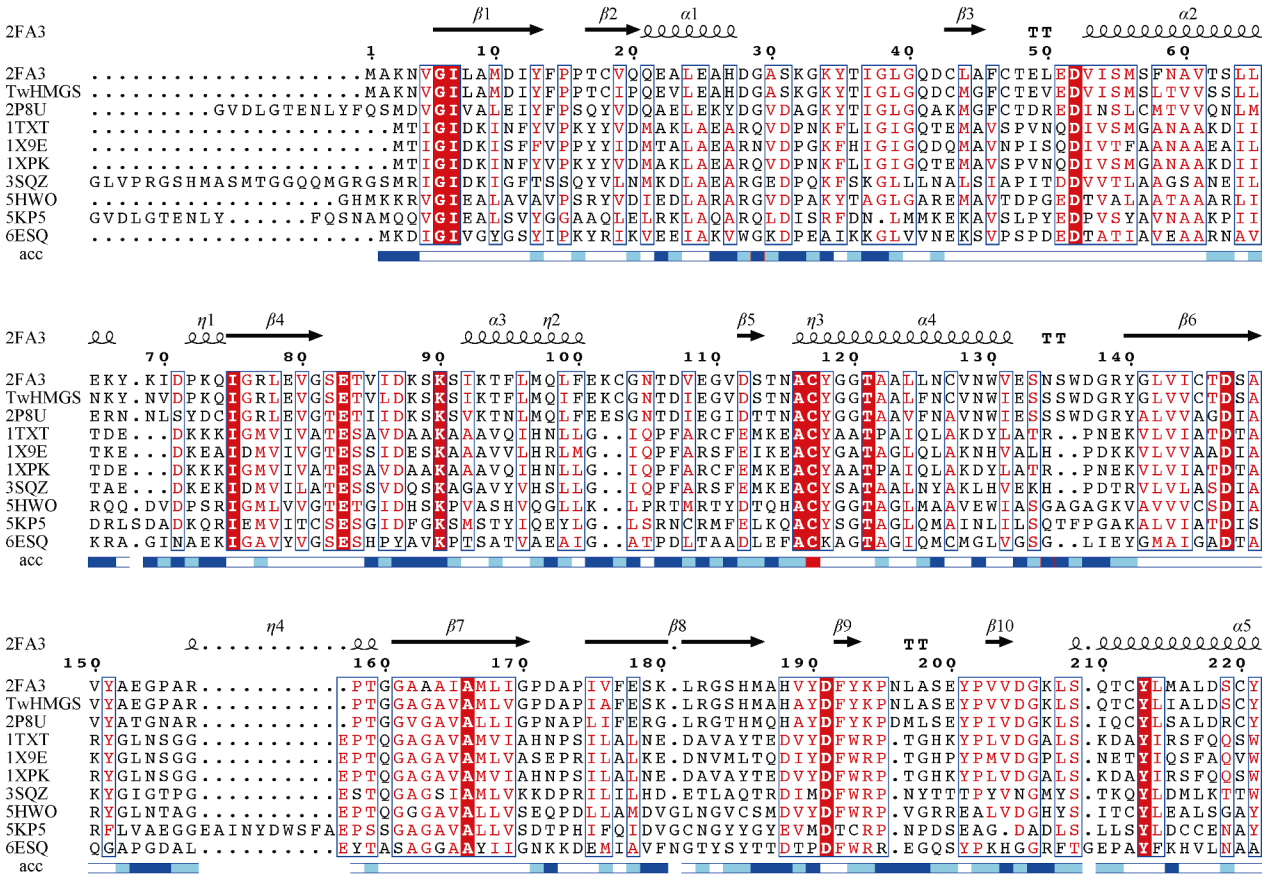

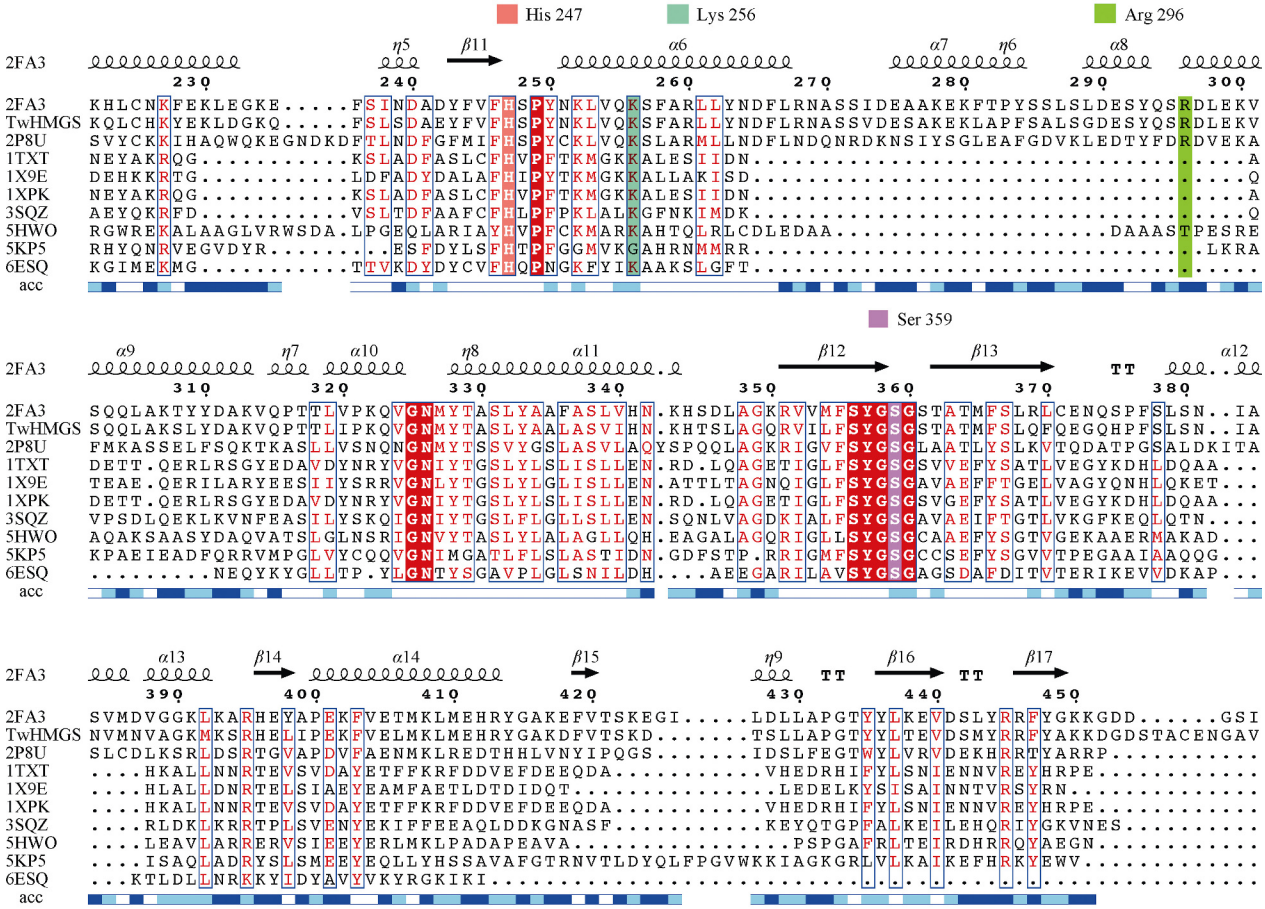


**Fig. 2 Sequence alignment and secondary structure of TwHMGS and nine HMGSs with reported crystal structures. The protein sequences are as follows. *Brassica juncea* (PDB: 2FA3), *Staphylococcus aureus* (PDB: 1TXT), *Enterococcus faecalis* (PDB: 1X9E); *Staphylococcus aureus* (strain MW2) (PDB: 1XPK), *Streptococcus mutans serotype c* (strain ATCC 700610/UA159) (PDB: 3SQZ), *Myxococcus xanthus* (strain DK 1622) (PDB: 5HWO), *Moorea producens* 3L (PDB: 5KP5), *Methanothermococcus thermolithotrophicus* (PDB: 6ESQ), *Homo sapiens* (PDB: 2P8U)**

Specific primers were designed to amplify the cDNA of each sample. The pH7WG2D and pH7WG2D−*TwHMGS*$_{OE}$ were identified *via* the Hyg fragment of 1787 bp, while pK7GWIWG2D and pK7GWIWG2D−*TwHMGS*$_{Ri}$ were verified by the Kan fragment of 1397 bp (Fig. 3). The electrophoresis bands were shown in Fig. 3C. These results indicated that the suspension cells were successfully transformed with the pH7WG2D−*TwHMGS*$_{OE}$, pK7GWIWG2D−*TwHMGS*$_{Ri}$, pH7WG2D and pK7GWIWG2D vectors, respectively.

*Expression analysis of TwHMGS and the related genes in the terpene biosynthetic pathway*

The relative transcription level of *TwHMGS* was determined by RT-qPCR. Compared to the suspension cells transformed with the empty vector, the overexpression group exhibited a 2-fold increase (Fig. 4A). Conversely, the expression of *TwHMGS* in the RNAi group was reduced to approximately 70% of the control (Fig. 4B).

Apart from the expression analysis of *TwHMGS*, we focused on the expression of genes in the MEP pathway and further downstream in the biosynthesis of terpene (Fig. 4).

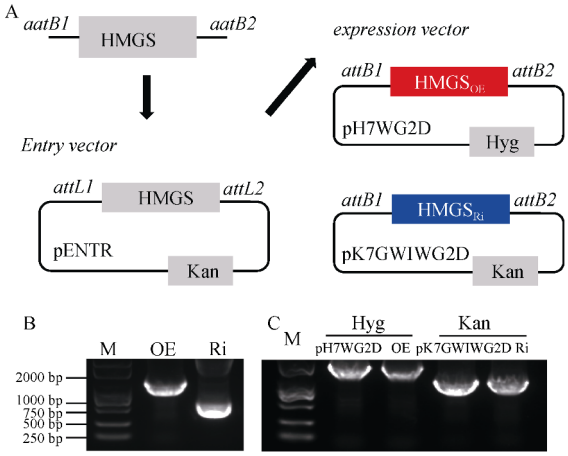


**Fig. 3 Agarose gel electrophoresis of target fragments. (A) Schematic diagram of vector construction. Hyg stands for the hygromycin resistance cassette, Kan for kanamycin. (B) OE: *TwHMGS* overexpression fragment (1398 bp), Ri: *Tw*HMGS RNAi fragment (515 bp). (C) Partial agarose gel electrophoresis of the Hyg fragment (1787 bp) and Kan fragment (1397 bp). OE stands for overexpression; Ri is RNAi**

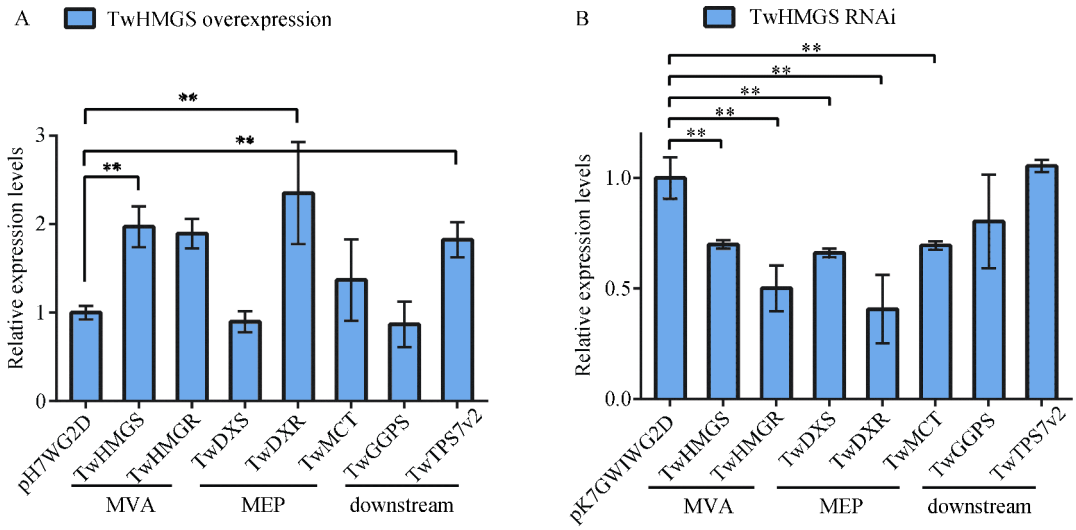


**Fig. 4 Expression analysis of related genes in overexpression and RNAi suspension cells. (A) Relative expression levels in the *TwHMGS* overexpression group with empty vector pH7WG2D as control. (B) Relative expression levels in the *TwHMGS* RNAi group with empty vector pK7GWIWG2D as control. The data represented the averages of five independent biological samples with three technical replicates. $^{**}P < 0.01$, $n = 5$. The difference between the means of two samples is tested by independent samples *t*-test method**

HMG-CoA reductase (HMGR) and HMGS are adjacent enzymes in the cytosolic MVA pathway. The HMGR converts HMG-CoA, the product of HMGS, to mevalonate. In the *TwHMGS* overexpression group, the *TwHMGR* mRNA was induced, reaching an approximately 1.9-fold high value that that of the control. In the RNAi group, the *TwHMGR* mRNA level decreased to about half that of the control (Fig. 4). The 1-deoxy-D-xylulose-5-phosphate synthase (DXS) and 1-deoxy-D-xylulose-5-phosphate reductoisomerase (DXR) are the first two rate-limiting enzymes in the plastidic MEP pathway. Additionally, 2-*C*-methyl-D-erythritol-4-phosphate cytidylyltransferase (MCT or IspD) is another key enzyme in the MEP pathway. The expression of *TwDXS*, *TwDXR* and *TwMCT* decreased in all RNAi suspension cells, whereas the levels of *TwDXS* and *TwMCT* in the overexpression group remained unaffected. Among these, the mRNA of *TwDXR* had the largest increment during *TwHMGS* overexpression (Fig. 4A). *TwTPS7v2* is the class I diterpene cyclase in the downstream pathway of terpene synthesis [25]. Approximately 1.8-fold increasing was observed in the expression of *TwTPS7v2* when *TwHMGS* was overexpressed (Fig. 4). The expression of *TwGGPS* did not change significantly during *TwHMGS* overexpression and RNAi.

*Accumulation of triptolide and celastrol in the suspension cells*

Triptolide and celastrol are pharmacologically active diterpene and triterpene natural products of *T. wilfordii*, respectively. We detected the content of triptolide and celastrol in the overexpression groups, RNAi groups and the control groups. The methanol extracts from independent samples were analyzed by UPLC. The chromatogram of triptolide and celastrol was shown in Figs. 5A and 5B, where peak 1 detected at 425 nm corresponded to triptolide and peak 2 detected at 219.5 nm to celastrol. The standard curve equations for quantifying triptolide and celastrol were $Y = 10\ 849X + 6075.8$ ($R^2 = 0.9964$) and $Y = 2678.4X - 261.29$ ($R^2 = 0.9998$), respectively. Overexpression of *TwHMGS* promoted the synthesis of triptolide by 2-fold and had no significant effect on the celastrol content compared to the control groups (Fig. 5C). In the RNAi and pK7GWIWG2D groups, the contents of triptolide were 5.51 ± 1.87 and 14.80 ± 2.17 $\mu g \cdot g^{-1}$, respectively, while those of celastrol were 41.50 ± 5.76 and 50.56 ± 10.95 $\mu g \cdot g^{-1}$. The limited culture time of the suspension cells that were transformed with expression vectors may be a bit short for the accumulation of celastrol. These results supported the vital function of TwHMGS in the biosynthesis of terpenes in *T. wilfordii* suspension cells.

*Ligand docking suggesting the key residues for catalysis*

The crystal structures of *Bj*HMGS in the apo-form and *Bj*HMGS in complex with acetyl-CoA exhibited an open-closed change of conformation [22]. Therefore, the structure of *Bj*HMGS in complex with acetyl-CoA structure was used as template to construct the three-dimensional homology model of TwHMGS. The values of GMQE and identity were 0.92% and 83.93%, respectively, which support the reliability of modeling. The overall structure of TwHMGS was composed of helices, sheets and loops, and as similar to the reported structures *Bj*HMGS and bacterial HMGS with the conserved *αβαβα* catalytic fold (Fig. 6A) [26-29]. Depending on the ligand docking result, the substrate acetyl-CoA and some residues, including the Arg296, Lys256, and His247, potentially existed mutual polar contacts excluding solvent. The His247 was reported to be a highly conserved site (Fig. 2), serving as a hydrogen donor in the deacetylation process of BjHMGS [22]. In TwHMGS, the distance between His-247 and the acetyl

oxygen atom was 2.9 Å, which may share the same mechanism reported for BjHMGS. The phosphate groups of acetyl-CoA were bound to basic residues, such as K256, K34 and R296 through electrostatic interactions (Fig. 6B). In addition, the CoA was anchored by an H-bond interaction between the adenine moiety and the hydroxyl side chain of Ser31 (Fig. 6B).

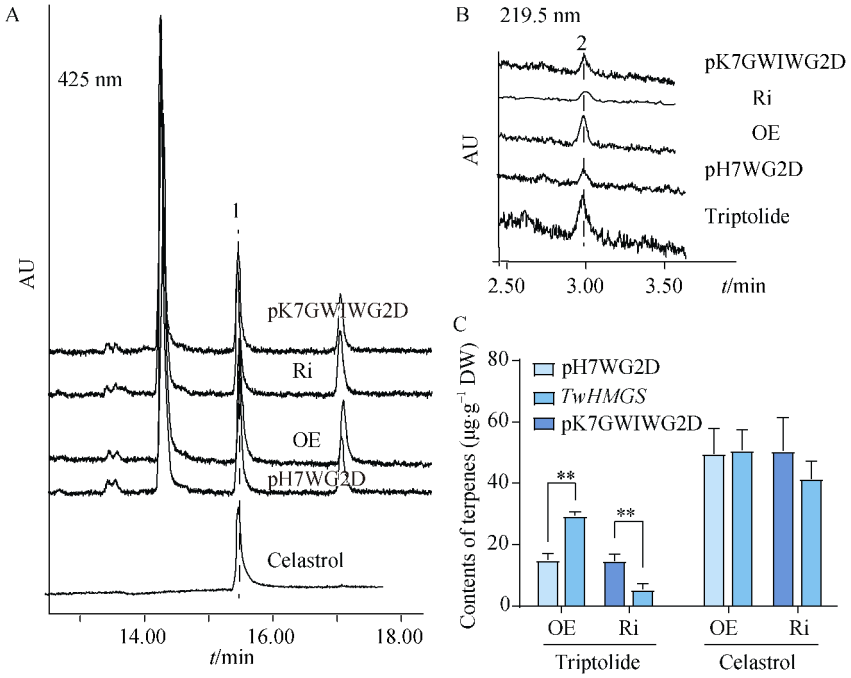


**Fig. 5 UPLC chromatograms and contents of triptolide and celastrol in *T. wilfordii* suspension cells after transformation with expression vectors. (A) UPLC chromatograms of samples and celastrol standard monitored at 425 nm. Peak 1: celastrol. (B) UPLC chromatograms of samples and triptolide standard monitored at 219.5 nm. Peak 2: triptolide. (C) The data represented the averages of five independent biological samples with three technical replicates. OE stands for overexpression; Ri is RNAi. $^{**}P < 0.01$, $n = 5$. The difference between the means of two samples is tested by independent samples *t*-test method**

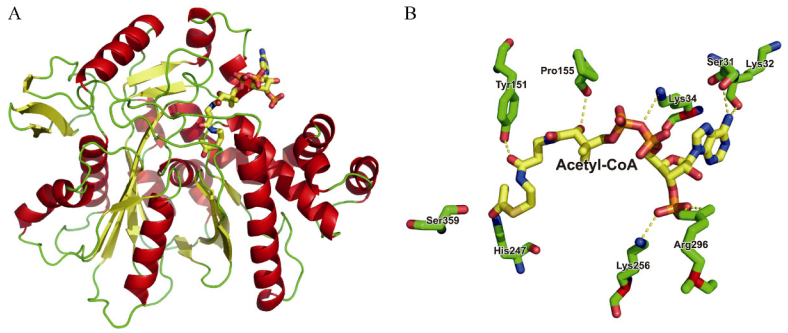


**Fig. 6 Ligand docking of acetyl-CoA in the active site of TwHMGS. (A) The overall structure of TwHMGS according to homology modeling with BjHMGS (PDB: 2FA3) as the template. The structure of TwHMGS is colored by secondary structure, red for helices, yellow for sheets and green for loops. The ligand acetyl-CoA is shown in stick. (B) Key residues around the acetyl-CoA are labeled, the yellow dotted line linkes the residues with potential polar contacts and the distances are less than 3.5 Å**

## Discussion

HMGS is the rate-limiting enzyme in the biosynthesis of isoprenoids, the C5 precursor of all terpenes. The crystal structures of HMGS from *Staphylococcus aureus* [26] and from *Brassica juncea* [22], in conjunction with site-directed mutagenesis studies, have revealed details of the mechanism of catalysis. The reaction catalyzed by HMGS consists of three steps namely acetylation, condensation and dehydration. We noticed that key residue R296 was not conserved among the seven bacteria including *Myxococcus xanthus* and *Enterococcus faecalis* (Fig. 2). Furthermore, the residue K256 of TwHMGS was not completely conserved in other HMGS, especially that from *Moorea producens* 3 L [30]. This phenomenon suggested that the residues may be responsible for some of the structural differences between bacterial and plant enzymes. Overexpression of *Brassica juncea* HMGS has been studied in *Arabidopsis*. The stigmasterol and sitosterol contents were significantly increased in leaves and seedlings of the overexpression lines [31]. A similar result was shown in Fig. 5.

However, neither the overexpression group nor the RNAi group showed significant changes in the accumulation of celastrol, the main bioactive triterpene of *T. wilfordii*. Generally speaking, triterpene biosynthesis relies on the cytosolic MVA pathway, while diterpene biosynthesis mainly uses the plastidial MEP pathway. However, metabolic cross-talk has been reported to occur between the MVA and MEP pathways, suggesting that isoprenoids flow between them [32-34]. This may explain the significant changes in the content of triptolide. In addition, the ratio of DMAPP/IPP influences the isoprene flux, and the differential expression of *TwHMGS* may interfere with the dynamic equilibrium between IPP and DMAPP [35], which we assumed to affect triptolide and celasol biosyntehsis. ZHANG *et al*. and SU *et al*. measured the terpenes of *T. wilfordii* suspension cells and found that the content of celastrol was higher than that of triptolide [25, 36-37]. The differential expression of single gene may prefer metabolite flux to compounds with low content. It was reported that the overexpression and RNAi of *TwDXR* and *TwIDI* affected the feedback regulation of other genes in the terpene synthesis pathway [36, 38]. The *TwHMGS* in our research just exhibited a synergistic regulation (Fig. 7).

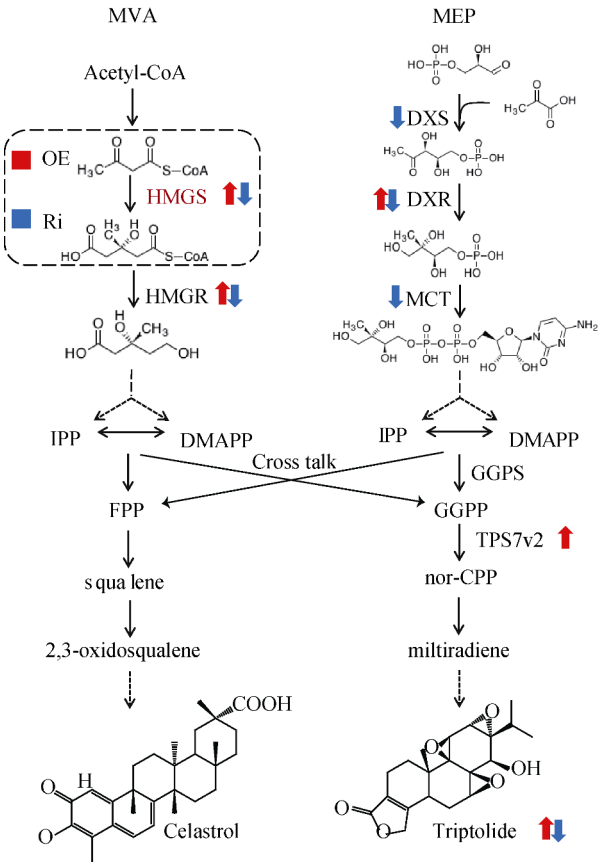


**Fig. 7 The relative genes in the biosynthesis pathway of triptolide and celastrol. OE indicates *TwHMGS* overexpression and Ri indicated TwHMGS RNAi. The upregulating genes and product are labeled with red arrows during *TwHMGS* overexpression. The downregulating genes and product are labeled with blue arrows during *TwHMGS* RNAi**

The His188 and Ser359 of *Bj*HMGS play a particularly important role in the catalytic activity of this enzyme [39]. The H188N mutation abrogated the substrate inhibition by acetoacetyl-CoA, while the S359A mutation highly increased *Bj*HMGS activity. We noticed that the Ser359 in TwHMGS was close to the substrate acetyl-CoA (Fig. 6B). Overexpression of the wild type *Bj*HMGS, the H188N mutant, S359A mutant and H188N/S359A double mutant in *Arabidopsis* improved both sterol production and stress tolerance [31]. Furthermore, the introduction of *Bj*HMGS: S359A into transgenic tomato obviously enhanced the α-tocopherol, carotenoid, squalene and phytosterol contents in the fruits [14].

## Conclusion

TwHMGS enzyme catalyzes the condensation of acetoacetyl-CoA to form HMG-CoA in the MVA pathway of terpene synthesis. RNAi and overexpression vectors targeting *TwHMGS* gene were respectively introduced into *T. wilfordii* suspension cells *via* biolistic-gun transformation and verified by PCR. *TwHMGS* overexpression in *T. wilfordii* not only elevated the expression of adjacent *TwHMGR*, but also *TwDXR* in the MEP pathway, and further downstream, the terpene cyclase gene *TwTPS7v2* related to diterpene biosynthesis was also upregulated. Meanwhile, a synergistic downregulation of *TwDXS*, *TwDXR*, *TwMCT* and *TwHMGR* occurred in the *TwHMGS* RNAi group (Fig. 7). Subsequently, changes in the diterpene end-product triptolide were investigated, providing an important reference for regulating the key genes in the biosynthesis pathway to generate pharmacologically active ingredients. The potential mechanism of HMGS catalytic activity was analyzed on the basis of molecular docking, exploring the binding state of TwHMGS in complex with acetyl-CoA.

## Acknowledgments

The authors acknowledge XIANG Yu-Hong in Capital Normal University for supporting SYBYL-based computing services.

## References

[1] Goldbach-Mansky R, Wilson M, Fleischmann R, *et al.* Comparison of *Tripterygium wilfordii* Hook F versus sulfasalazine in the treatment of rheumatoid arthritis: a randomized trial [J]. *Ann Intern Med*, 2009, **151**(4): 229-240, w249-251.

[2] Wang M, Huang J, Fan H, *et al.* Treatment of rheumatoid arthritis using combination of methotrexate and tripterygium glycosides tablets-A quantitative plasma pharmacochemical and pseudotargeted metabolomic approach [J]. *Front Pharmacol*, 2018, **9**: 1051.

[3] He QL, Minn I, Wang Q, *et al.* Targeted delivery and sustained antitumor activity of triptolide through glucose conjugation [J]. *Angew Chem Int Ed Engl*, 2016, **55**(39): 12035-12039.

[4] Liu J, Lee J, Salazar Hernandez MA, *et al.* Treatment of obesity with celastrol [J]. *Cell*, 2015, **161**(5): 999-1011.

[5] Hu M, Luo Q, Alitongbieke G, *et al.* Celastrol-induced Nur77 interaction with TRAF2 alleviates inflammation by promoting mitochondrial ubiquitination and autophagy [J]. *Mol Cell*, 2017, **66**(1): 141-153.

[6] Dandawate PR, Subramaniam D, Jensen RA, *et al.* Targeting cancer stem cells and signaling pathways by phytochemicals: Novel approach for breast cancer therapy [J]. *Semin Cancer Biol*, 2016, **40-41**: 192-208.

[7] Kuzuyama T, Seto H. Two distinct pathways for essential metabolic precursors for isoprenoid biosynthesis [J]. *Proc Jpn Acad Ser B Phys Biol Sci*, 2012, **88**(3): 41-52.

[8] Lombard J, Moreira D. Origins and early evolution of the mevalonate pathway of isoprenoid biosynthesis in the three domains of life [J]. *Mol Biol Evol*, 2011, **28**(1): 87-99.

[9] Puisac B, Marcos-Alcalde I, Hernandez-Marcos M, *et al.* Human mitochondrial HMG-CoA synthase deficiency: Role of enzyme dimerization surface and characterization of three new patients [J]. *Int J Mol Sci*, 2018, **19**(4): E1010.

[10] Meng X, Song Q, Ye J, *et al.* Characterization, function, and transcriptional profiling analysis of 3-hydroxy-3-methylglutaryl-CoA synthase gene (GbHMGS1) towards stresses and exogenous hormone treatments in *Ginkgo biloba* [J]. *Molecules*, 2017, **22**(10): E1706.

[11] Peralta-Yahya PP, Ouellet M, Chan R, *et al.* Identification and microbial production of a terpene-based advanced biofuel [J]. *Nat Commun*, 2011, **2**: 483.

[12] Liu YJ, Zhao YJ, Zhang M, *et al.* Cloning and characterisation of the gene encoding 3-hydroxy-3-methylglutaryl-CoA synthase in *Tripterygium wilfordii* [J]. *Molecules*, 2014, **19**(12): 19696-19707.

[13] Lee AR, Kwon M, Kang MK, *et al.* Increased sesqui- and triterpene production by co-expression of HMG-CoA reductase and biotin carboxyl carrier protein in tobacco (*Nicotiana benthamiana*) [J]. *Metab Eng*, 2019, **52**: 20-28.

[14] Liao P, Chen X, Wang M, *et al.* Improved fruit alpha-tocopherol, carotenoid, squalene and phytosterol contents through manipulation of *Brassica juncea* 3-HYDROXY-3-METHYLGLUTARYL-COA SYNTHASE1 in transgenic tomato [J]. *Plant Biotechnol J*, 2018, **16**(3): 784-796.

[15] Meister G, Tuschl T. Mechanisms of gene silencing by double-stranded RNA [J]. *Nature*, 2004, **431**(7006): 343-349.

[16] Miziorko HM, Clinkenbeard KD, Reed WD, *et al.* 3-Hydroxy-3-methylglutaryl coenzyme A synthase. Evidence for an acetyl-*S*-enzyme intermediate and identification of a cysteinyl sulfhydryl as the site of acetylation [J]. *J Biol Chem*, 1975, **250**(15): 5768-5773.

[17] Tong Y, Su P, Zhao Y, *et al.* Molecular cloning and characterization of DXS and DXR genes in the terpenoid biosynthetic pathway of *Tripterygium wilfordii* [J]. *Int J Mol Sci*, 2015, **16**(10): 25516-25535.

[18] Zhao Y, Zhang Y, Su P, *et al.* Genetic transformation system for woody plant *Tripterygium wilfordii* and its application to product natural celastrol [J]. *Front Plant Sci*, 2017, **8**: 2221.

[19] Tong YR, Su P, Guan HY, *et al.* Eudesmane-type sesquiterpene diols directly synthesized by a sesquiterpene cyclase in *Tripterygium wilfordii* [J]. *Biochem J*, 2018, **475**(17): 2713-2725.

[20] Boucher Y, Doolittle WF. The role of lateral gene transfer in the evolution of isoprenoid biosynthesis pathways [J]. *Mol Microbiol*, 2000, **37**(4): 703-716.

[21] Kai G, Li S, Wang W, *et al.* Molecular cloning and expression analysis of a gene encoding 3-hydroxy-3-methylglutaryl-CoA synthase from *Camptotheca acuminata* [J]. *Rus J Plant Physiol*, 2013, **60**(1): 131-138.

[22] Pojer F, Ferrer JL, Richard SB, *et al.* Structural basis for the design of potent and species-specific inhibitors of 3-hydroxy-3-methylglutaryl CoA synthases [J]. *Proc Natl Acad Sci U S A*, 2006, **103**(31): 11491-11496.

[23] Fu Z, Runquist JA, Forouhar F, *et al.* Crystal structure of human 3-hydroxy-3-methylglutaryl-CoA lyase insights into catalysis and the molecular basis for hydroxymethylglutaric aciduria [J]. *J Biol Chem*, 2006, **281**(11): 7526-7532.

[24] Skaff DA, Ramyar KX, McWhorter WJ, *et al.* Biochemical and structural basis for inhibition of Enterococcus faecalis hydroxymethylglutaryl-CoA synthase, mvaS, by hymeglusin [J]. *Biochemistry*, 2012, **51**(23): 4713-4722.

[25] Su P, Guan H, Zhao Y, *et al.* Identification and functional characterization of diterpene synthases for triptolide biosynthesis from *Tripterygium wilfordii* [J]. *Plant J*, 2018, **93**(1): 50-65.

[26] Theisen MJ, Misra I, Saadat D, *et al.* 3-Hydroxy-3-methylglutaryl-CoA synthase intermediate complex observed in "real-time" [J]. *Proc Natl Acad Sci U S A*, 2004, **101**(47): 16442-16447.

[27] Steussy CN, Vartia AA, Burgner JW, *et al.* X-ray crystal structures of HMG-CoA synthase from Enterococcus faecalis and a complex with its second substrate/inhibitor acetoacetyl-CoA [J]. *Biochemistry*, 2005, **44**(43): 14256-14267.

[28] Steussy CN, Robison AD, Tetrick AM, *et al.* A structural limitation on enzyme activity: the case of HMG-CoA synthase [J]. *Biochemistry*, 2006, **45**(48): 14407-14414.

[29] Vogeli B, Engilberge S, Girard E, *et al.* Archaeal acetoacetyl-CoA thiolase/HMG-CoA synthase complex channels the intermediate *via* a fused CoA-binding site [J]. *Proc Natl Sci U S A*, 2018, **115**(13): 3380-3385.

[30] Maloney FP, Gerwick L, Gerwick WH, *et al.* Anatomy of the beta-branching enzyme of polyketide biosynthesis and its interaction with an acyl-ACP substrate [J]. *Proc Natl Acad Sci U S A*, 2016, **113**(37): 10316-10321.

[31] Wang H, Nagegowda DA, Rawat R, *et al.* Overexpression of *Brassica juncea* wild-type and mutant HMG-CoA synthase 1 in Arabidopsis up-regulates genes in sterol biosynthesis and enhances sterol production and stress tolerance [J]. *Plant Biotechnol J*, 2012, **10**(1): 31-42.

[32] Mendoza-Poudereux I, Kutzner E, Huber C, *et al.* Metabolic cross-talk between pathways of terpenoid backbone biosynthesis in spike lavender [J]. *Plant Physiol Biochem*, 2015, **95**: 113-120.

[33] Opitz S, Nes WD, Gershenzon J. Both methylerythritol phosphate and mevalonate pathways contribute to biosynthesis of each of the major isoprenoid classes in young cotton seedlings [J]. *Phytochemistry*, 2014, **98**: 110-119.

[34] Hemmerlin A, Hoeffler JF, Meyer O, *et al.* Cross-talk between the cytosolic mevalonate and the plastidial methylerythritol phosphate pathways in tobacco bright yellow-2 cells [J]. *J Biol Chem*, 2003, **278**(29): 26666-26676.

[35] Weise SE, Li Z, Sutter AE, *et al.* Measuring dimethylallyl diphosphate available for isoprene synthesis [J]. *Anal Biochem*, 2013, **435**(1): 27-34.

[36] Zhang Y, Zhao Y, Wang J, *et al.* Overexpression and RNA interference of TwDXR regulate the accumulation of terpenoid active ingredients in *Tripterygium wilfordii* [J]. *Biotechnol Lett*, 2018, **40**(2): 419-425.

[37] Su P, Cheng Q, Wang X, *et al.* Characterization of eight terpenoids from tissue cultures of the Chinese herbal plant, *Tripterygium wilfordii*, by high-performance liquid chromatography coupled with electrospray ionization tandem mass spectrometry [J]. *Biomed Chromatogr*, 2014, **28**(9): 1183-1192.

[38] Wang J, Zhao Y, Zhang Y, *et al.* Overexpression and RNAi-mediated downregulation of TwIDI regulates triptolide and celastrol accumulation in *Tripterygium wilfordii* [J]. *Gene*, 2018, **679**: 195-201.

[39] Nagegowda DA, Bach TJ, Chye ML. *Brassica juncea* 3-hydroxy-3-methylglutaryl (HMG)-CoA synthase 1: expression and characterization of recombinant wild-type and mutant enzymes [J]. *Biochem J*, 2004, **383**(Pt. 3): 517-527.

**Cite this article as:** TONG Yu-Ru, ZHANG Yi-Feng, ZHAO Yu-Jun, HU Tian-Yuan, WANG Jia-Dian, HUANG Lu-Qi, GAO Wei. Differential expression of the *TwHMGS*[0] gene and its effect on triptolide biosynthesis in *Tripterygium wilfordii* [J]. *Chin J Nat Med*. 2019, **17**(7): 575-584.

**HUANG Lu-Qi, Academician of Chinese Academy of Engineering, China Academy of Chinese Medical Sciences**

HUANG Lu-Qi is the president of China Academy of Chinese Medical Sciences, a leading researcher, a group leader of the experts guiding group for the national survey on Chinese Medicinal Material Resources, the head of Chinese Medicinal Material Resources Innovation Team of Key Area issued by Ministry of Science and Technology, former Chief Scientist of national 973 plan project. He is concurrently as the chairman of Chinese Materia Medica Identification Committee, which is the branch of China Association of Chinese Medicine, and the director of the Medicinal Plants and Plant Medicine Professional Board of Botanical Society of China, and the Chairman of the Technical Committee of Chinese Medicinal Materials Seeds (Seedling) Standardization.

He won the second prize of State Science and Technology Progress Award as the first completed person for three times. He has published more than 500 professional papers on domestic and international top-level publications, obtained seven patents, and edited 12 books as Editor-in-Chief. He was awarded the China Academy of Engineering—Guang Hua Engineering Science and Technology Prize (youth award), “The State Special Support Plan”—National Millions of Talents Project, Science and Technology Award for Chinese Youth, and the Supervisor Award of the National Outstanding Doctoral Dissertations.

**Prof. GAO Wei, Ph.D, Capital Medical University**

GAO Wei is a professor of Capital Medical University. He was selected into the Chang Jiang Scholars Program by the Ministry of Education and the National High-level Personnel of Special Support Program. He was funded by National Natural Science Foundation for OutstandingYouth Foundation, China. Dr. Gao’s research interests focus on the study of natural medicinal resources and molecular pharmacognosy, especially the regulation of medicinal active component gene of the terpenoids and the synthetic biology research. His group revealed the metabolic pathways and networks of tanshinones, triptolide and celastrol and investigated the function of enzymes and the mechanism.

He has published over 80 papers, among which 40 SCI papers were published in JACS, New Phytologist, Organic letters, etc. He also gained five provincial awards and 18 patents. His research has been supported by several grants (National Natural Science Foundation for Outstanding Youth Foundation, the National High-level Personnel of Special Support Program, and 863 Program, etc). Moreover, he is a member of TCM Identification Branch of China Association of Chinese Medicine, TCM Resources Branch of China Association of Chinese Medicine and China Journal of Chinese Materia Medica, etc.